neuralized Encodes a Peripheral Membrane Protein Involved in Delta Signaling and Endocytosis

Elias Pavlopoulos,[1,2,6] Chrysoula Pitsouli,[1,2,6]
Kristin M. Klueg,[3] Marc A.T. Muskavitch,[4]
Nicholas K. Moschonas,[1,2]
and Christos Delidakis[1,2,5]
[1] Institute of Molecular Biology and Biotechnology
Foundation for Research and Technology Hellas
[2] Department of Biology
University of Crete
711 10 Heraklion, Crete
Greece
[3] Department of Biology
Indiana University
Bloomington, Indiana 47405
[4] Biology Department
Boston College
Chestnut Hill, Massachusetts 02467

Summary

Activation of the Notch (N) receptor involves an intracellular proteolytic step triggered by shedding of the extracellular N domain (N-EC) upon ligand interaction. The ligand Dl has been proposed to effect this N-EC shedding by transendocytosing the latter into the signal-emitting cell. We find that Dl endocytosis and N signaling are greatly stimulated by expression of *neuralized* (*neur*). *neur* inactivation suppresses Dl endocytosis, while its overexpression enhances Dl endocytosis and Notch-dependent signaling. We show that *neur* encodes an intracellular peripheral membrane protein. Its C-terminal RING domain is necessary for Dl accumulation in endosomes, but may be dispensable for Dl signaling. The potent modulatory effect of Neur on Dl activity makes Neur a candidate for establishing signaling asymmetries within cellular equivalence groups.

Introduction

Notch (N) signaling mediates a multitude of developmental processes in metazoans, most of which are related to cell fate acquisition. Although considerable progress has been made in elucidating the molecular mechanism of Notch signaling (reviewed in Artavanis-Tsakonas et al., 1999; Mumm and Kopan, 2000), a number of puzzling questions remain. One concerns the spatial regulation of the signal. In *Drosophila*, the N receptor is relatively ubiquitously expressed. Its ligands, Delta (Dl) and Serrate (Ser), though displaying more dynamic expression, are expressed in broad cellular ensembles (Kooh et al., 1993; Speicher et al., 1994). Only a subset of these cells receives the signal at any time, as reflected by the expression of transcriptional targets of N, such as *Enhancer of split* (*E(spl)*) or *vestigial* (*vg*). These observations raise the question of what it is that determines

which cells send and which cells receive signal (Baker, 2000). In the case of wing dorso-ventral (DV) boundary establishment, this can be accounted for in part by differential glycosylation of N by Fringe (Fng; Blair, 2000) and in part by a transcriptional threshold imposed on N target genes by the repressor Nubbin (Neumann and Cohen, 1998). In the case of lateral inhibition, it has been proposed that nascent neural/vein precursors upregulate *Dl* transcription while repressing *N* and vice versa for their neighbors, making the former better signal emitters and the latter better signal receivers (Heitzler and Simpson, 1991). This reciprocal transcriptional regulation has been experimentally substantiated in the case of vein lateral inhibition (de Celis et al., 1997; Huppert et al., 1997), but not in proneural fields, where *Dl* and *N* are simultaneously downregulated in the signal-emitting cell (Baker and Yu, 1998; Fehon et al., 1991; Kooh et al., 1993).

A second puzzling question regards the actual mechanism of N activation by its ligands. It has recently been shown that a crucial extracellular event during N activation is proteolysis close to the cell membrane followed by shedding of the large N extracellular domain (Brou et al., 2000; Rand et al., 2000; Struhl and Adachi, 2000). Ligand binding should somehow precipitate these events, but the mechanism remains unclear. A possible way to achieve ectodomain shedding has been proposed by Parks et al. (2000), who showed that Dl can trigger transendocytosis of the N-EC, but not the N intracellular (N-IC), domain. Indeed, the role of endocytosis in N signaling has remained something of a mystery. A mutation in *shibire* (*shi*), the gene encoding the GTPase dynamin, which mediates pinching off of coated pits, phenocopies *N* mutations (Poodry, 1990). However, mosaic analysis has not been able to pinpoint whether *shi* is needed in the sending or the receiving cell; it seems to be required in both (Seugnet et al., 1997). This possibly reflects the pleiotropic roles of dynamin in membrane reorganization processes, including secretion from the Golgi (McNiven et al., 2000). From genetic studies it appears that *shi* is not required for the constitutive activity of dominant N truncations that lack the ectodomain, even if they are membrane tethered (Seugnet et al., 1997; Struhl and Adachi, 2000). This places the role of dynamin-mediated processes (including endocytosis) upstream of or during N extracellular cleavage and ectodomain shedding.

Our analysis of *neuralized* (*neur*), a classic Notch pathway ("neurogenic") gene, has revealed that it stimulates Dl endocytosis. *neur* loss-of-function (lof) blocks Notch signaling during lateral inhibition and produces embryonic lethality with the same neurogenic phenotype as *N* lof mutations (Lehman et al., 1983). *neur* encodes a membrane-associated protein with two novel internal repeats and a C-terminal RING domain (Lai and Rubin, 2001; Price et al., 1993). We show that Neur can cause dramatic relocalization of Dl from the cell membrane to intracellular vesicles and concomitantly enhance Dl signaling to N. We discuss how Neur activity, coupled

[5] Correspondence: delidaki@imbb.forth.gr
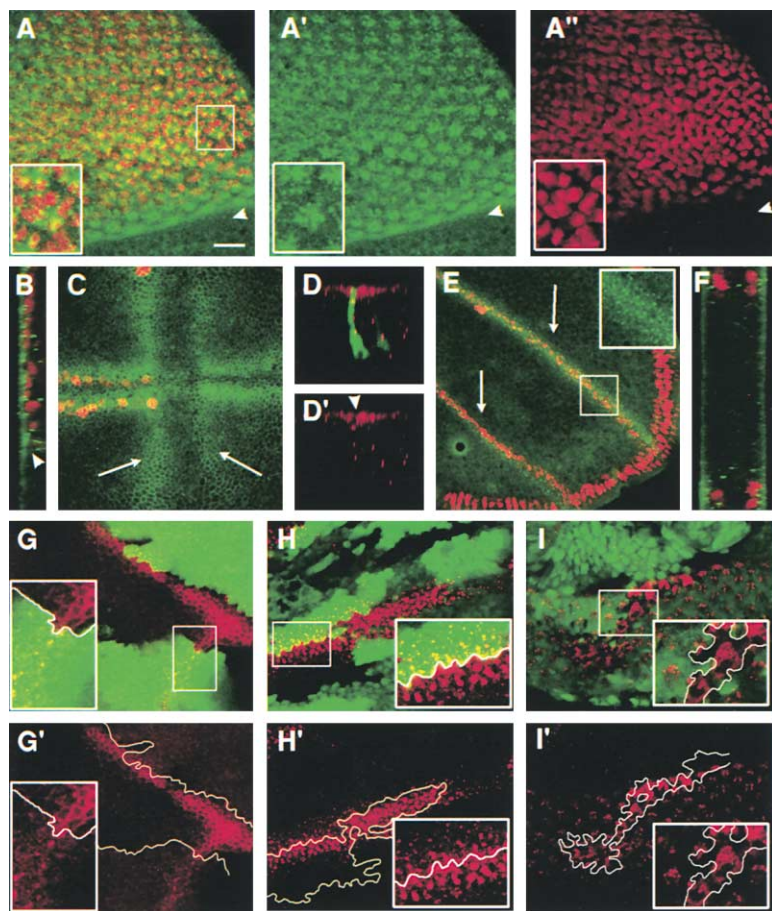[6] These authors contributed equally to this work.

Figure 1. *neur* Is Required for Dl Endocytosis

(A–C, E, and F) Dl accumulation (green) in Neur-expressing cells (red, nuclear β-galactosidase from *neur^{A101}-lacZ*) in eye and wing disks.

(D) Dl accumulation (red) in SOPs (green cytoplasmic EGFP from *neur-Gal4;UAS-EGFP*).

(A and B) Third instar eye disk ([A], posterior upward) and its corresponding cross-section ([B], apical left) display vesicular accumulation of Dl. Dl only (A′); β-galactosidase (*neur^{A101}-lacZ*) only (A′′). The arrowhead indicates morphogenetic furrow.

(C) Third instar wt wing disk (anterior at left, dorsal upward). Dl is pericellular both in the wing margin (anterior half marked by *neur^{A101}-lacZ*-positive SOPs) and in the vein primordia (arrows).

(D) Cross-section of third instar wing margin; apical is up. The apical aspect of the most intensely labeled SOP exhibits reduced Dl (red) accumulation, more clearly evident as a gap (arrowhead) in D′ (red channel only).

(E) Thirty hour APF pupal wing. *neur^{A101}-lacZ* marks the wing margin and the veins. At this stage, there is no Dl immunoreactivity at the wing margin, but veins (arrows) contain vesicular Dl. Inset: green channel only of boxed region at twice the magnification.

(F) The cross-section corresponding to (E) reveals vesicular Dl accumulation and the absence of apical Dl. Unlike the monolayer epithelium shown in (B), the pupal wing consists of two layers: the apposed dorsal and ventral wing blade epithelia. Apical sides are outward.

(G–I) Dl accumulation (red, shown separately in [G′]–[I′]) in mutant tissues, identified by the absence of β-galactosidase (green in [G]) or GFP (green in [H] and [I]).

(G) Thirty hour APF veins; *neur^1* clone. Dl exhibits membrane localization in the mutant tissue.

(H) Thirty hour APF veins; *E(spl)^{b32.2}* clones. Dl is still internalized in the mutant tissue. Note also increased Dl expression, presumably due to relief of repression by E(spl).

(I) Third instar eye disk; *neur* clones. As in (G), Dl is distinctly pericellular within the clone.

The scale bars indicate 10 μm in (A–D) and (F), 20 μm in (E), and 14 μm in (G–I).

Insets show corresponding boxed regions at twice the magnification.

with its documented preferential expression in signal-emitting cells (Boulianne et al., 1993; Huang et al., 1991), might generate asymmetries in N signaling.

Results

Neur Influences Dl Subcellular Localization

Dl, a transmembrane ligand of N, is found either on the apical side of the cell membrane or in more basally located intracellular particles that appear to be endocytic vesicles (Kooh et al., 1993). We noticed that increased Dl internalization occurs in tissues that express *neur*, such as the invaginating embryonic mesoderm (Kooh et al., 1993). We found that this correlation holds in many tissues. In the third instar larval eye disk, *neur* is expressed in differentiating cells posterior to the furrow, in which Dl accumulates in a number of large punctate structures (Parks et al., 1995; Figures 1A and 1B). In contrast, most third instar wing disk cells do not express *neur*, and Dl displays a pronounced pericellular distribution with little intracellular staining (Figure 1C). The only wing disk cells that express *neur* are the sensory organ precursors (SOPs), which exhibit little or no

apical membrane Dl (Kooh et al., 1993), and instead contain a number of intracellular puncta (Figure 1D). *Dl* is also expressed in the wing proveins. In the third larval instar as well as during early pupal stages, provein cells do not express *neur* and exhibit pericellular Dl (Figure 1C). From about 24 hr after puparium formation (APF), central provein cells express *neur^{A101}-lacZ*, and at the same time Dl protein distribution switches to a vesicular pattern (Figures 1E and 1F; Huppert et al., 1997).

To determine whether this correlation between *neur* expression and Dl internalization was causal, we assayed the localization of Dl in a *neur* lof genetic background. *neur^1* clones were analyzed in late larval eyes and late pupal wings (30 hr APF), tissues in which Dl is normally seen exclusively in internalized vesicles. Mutant cells displayed increased apical pericellular Dl (Figures 1G and 1I) with only residual intracellular staining, suggesting a defect in internalization. As a control, we studied clones of a deficiency for the *E(spl)* locus, which is involved in lateral inhibition but acts downstream of the N signal. Unlike their *neur^1* counterparts, late pupal proveins bearing *E(spl)* null clones still internalized Dl and displayed no pericellular immunoreactivity (Figure
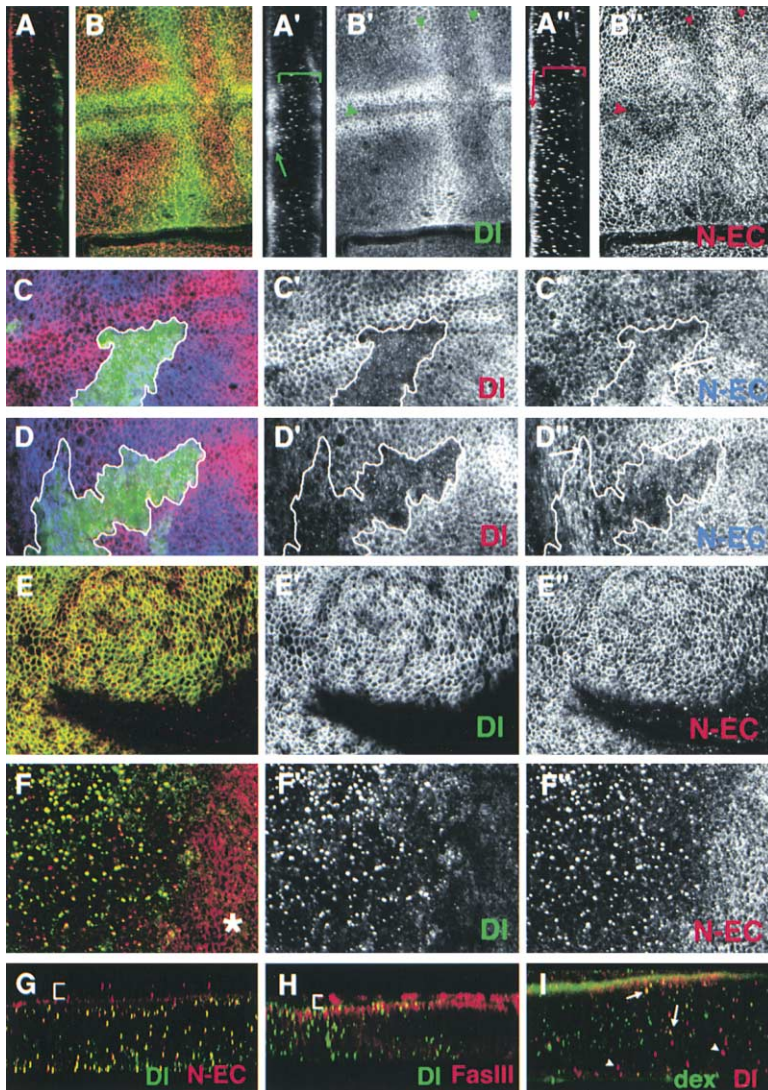
Figure 2. Ectopic Neur Stimulates Dl Internalization

(A and B) Dl (green, shown separately in [A'] and [B']) and N-EC (red, shown separately in [A''] and [B'']) accumulation in a wt wing disk. (A) Cross-section through the DV boundary (middle) and an adjacent vein (lower); apical is to the left. N and Dl both exhibit apical localization (arrows in [A'] and [A'']), as well as accumulation in internalized vesicles (brackets in [A'] and [A'']). Within regions of Dl expression, N and Dl colocalize in the apical cell membrane and in vesicles (yellow vesicles in [A]).

(B) Horizontal section, showing the expression pattern of Dl and N. Note lower levels of N at DV boundary (large arrowhead) and proveins (small arrowheads), due to transcriptional regulation.

(C and D) Dl (red, shown separately in [C'] and [D']) and N-EC (blue, shown separately in [C''] and [D'']) in FLP-out clones of *neur* overexpression, marked by GFP (green). Neur overexpression overlapping a Dl stripe at the wing margin (C) or provein (D) stimulates Dl and N-EC internalization (seen in these apical slices as loss of apical pericellular staining). However, N pericellular accumulation is not altered in parts of the clones that do not overlap with Dl stripes (arrows in [C''] and [D'']).

(E) Detail of an *omb-Gal4; UAS-Dl* wing pouch. Both ectopic Dl (green, [E']) and endogenous N-EC (red, [E'']) accumulate on the apical plasma membrane.

(F) Detail of an *omb-Gal4; UAS-Dl UAS-neur* wing pouch. Dl (green, [F']) and N-EC (red, [F'']) colocalize in intracellular vesicles (yellow in [F]) and are absent from the plasma membrane. For comparison, cells outside the *omb-Gal4* expression domain (asterisk) contain membrane N (and no Dl).

(G) Cross-section of an *omb-Gal4; UAS-Dl UAS-neur* disk (apical at top), stained as in (E) and (F). The bracket indicates the extent of the peripodial membrane which lies above the disk epithelium and expresses N, but no Dl. For the most part N and Dl colocalize within large vesicles along the apical-basal axis of the epithelium (yellow).

(H) Cross-section of an *omb-Gal4; UAS-Dl UAS-neur* wing pouch stained for Dl (green) and FasIII (red). FasIII is ubiquitously expressed and marks a subapical domain on both the peripodial membrane (brackets) and the epithelium. Internalized Dl vesicles within the *omb-Gal4* domain (left half) do not contain FasIII, implying that Neur does not stimulate FasIII internalization.

(I) Cross-section of an *omb-Gal4; UAS-Dl UAS-neur* wing pouch that has been incubated with fluorescein-dextran (green) to mark early endocytic vesicles, and stained for Dl (red). Many of the Dl vesicles are marked with fluorescein-dextran (some indicated by arrows), suggestive of endocytic provenance. Other Dl vesicles are dextran-negative (arrowheads); these more basally located structures do label with fluorescein-dextran after a 30–60 min chase (data not shown), suggesting that they belong to a later endosomal compartment.

1H). Similar effects on Dl subcellular localization were observed in *neur¹* embryos (data not shown). It therefore appears that *neur* lof blocks Dl internalization.

If Neur is needed to stimulate Dl internalization, then ectopic expression of *neur* might induce Dl relocalization in tissues in which it normally resides on the plasma membrane, such as the wing disk (Figures 1C, 2A, and 2B). Indeed, ectopically expressing a *UAS-neur* transgene at uniform levels in clones of larval wing disk cells (using the FLP-out technique; see Experimental Procedures) resulted in Dl internalization (Figures 2C and 2D). The apparent loss of pericellular Dl was not transcriptional because *UAS-neur* had no effect on a *Dl-lacZ* reporter (data not shown), while it induced Dl internalization even when *Dl* was ectopically coexpressed (Figures 2E and 2F).

While *UAS-Dl* expression alone targeted the protein to the apical plasma membrane, virtually no Dl immunoreactivity remained apical when *UAS-neur* was coexpressed. Instead, Dl relocalized to a multitude of vesicles found at various levels along the apical-basal axis (Figures 2F and 2G; see Supplemental Figure S1 [complementing Figure 2] at http://www.developmentalcell.com/cgi/content/full/1/6/807/DC1). That these belong to the endocytic compartment was confirmed by marking the latter with fluorescent dextran; dextran and Dl immunoreactivity colocalized in early (Figure 2I) and late endosomes. Localization of Fasciclin III, an apical transmembrane protein that does not participate in N signaling, did not change upon *neur* overexpression (Figure 2H).

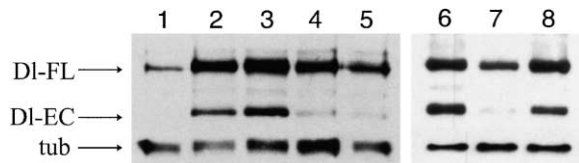In regions within which *Dl* and *N* are expressed, *neur*

Figure 3. *neur* Expression Downregulates Dl Protein Levels in Wing Disks

Wing disk extracts were analyzed by Western blot for Dl protein and for β-tubulin (tub) as a loading control. Dl-FL and Dl-EC are the full-length and extracellular cleavage product, respectively. Lanes 1–5 are from one experiment and lanes 6–8 from another. Lane 1: wt; lanes 2 and 3: *omb-Gal4; UAS-Dl UAS-GFP*; lanes 4, 5, and 7: *omb-Gal4; UAS-Dl UAS-neur*; lane 6: *omb-Gal4; UAS-Dl*; lane 8: *omb-Gal4; UAS-Dl UAS-neurΔRING-GFP*.

expression induced Dl-N-EC cointernalization, consistent with formation of a Dl-N-EC complex (Figures 2C and 2D). In regions within which *N* alone is expressed, *neur* expression did not affect N-EC subcellular localization (arrows in Figures 2C and 2D), suggesting that Dl-N cointernalization in the former regions does not reflect a direct effect of Neur on N. As observed for Dl, the effect of Neur on N is posttranscriptional because *UAS-neur* expression did not affect expression of an *N-lacZ* enhancer trap (data not shown). In wild-type wing disks and in disks expressing *UAS-Dl* alone, the few internalized Dl vesicles observed were positive for N-EC, while most N-EC immunoreactivity was at the membrane (where Dl also resides) and in additional Dl-negative vesicles (Figure 2A). In contrast, coexpression of *Dl* and *neur* led to substantial internalization of endogenous N, with most N-EC immunoreactivity found colocalizing with the Dl vesicles (Figure 2G; Supplemental Figure S1).

Neur Activity Decreases Dl Protein Levels Posttranscriptionally

As Neur appears to stimulate internalization of Dl and N, we asked whether this might be accompanied by a change in the overall levels or the pattern of proteolytic processing of either protein. Dl exists in two major isoforms, a full-length and an extracellularly cleaved one (Klueg et al., 1998; Qi et al., 1999). In protein extracts of late larval wing disks, the full-length Dl isoform predominated, with cleaved Dl present at roughly 10-fold lower levels than full-length. The effect of Neur was studied using *omb-Gal4* (broad wing pouch pattern) to overexpress *UAS-Dl* with either a neutral second transgene, *UAS-GFP* (to keep the total dosage of *UAS* targets constant), or with *UAS-neur*. As *Dl* is expressed from a heterologous promoter in these experiments, the effects observed must be posttranscriptional. Comparing *Dl+neur* with *Dl+GFP* expression revealed lower amounts of both Dl isoforms (Figure 3) in the former case. From densitometry analysis, we concluded that the total Dl levels were reduced by about 3-fold upon *Dl-neur* coexpression. Furthermore, whereas cleaved Dl accounted for about a third of the total Dl protein in control *omb-Gal4; UAS-Dl UAS-GFP* disks, its abundance dropped sharply upon coexpression of *neur*, to account for only one-tenth of the total Dl protein. This implies that Neur posttranscriptionally downregulates the levels of Dl, especially of the cleaved isoform. This probably reflects

increased turnover of Dl after internalization. The same samples of wing disks were analyzed for the presence of N isoforms using two antibodies, one against an extracellular and one against an intracellular epitope. No major changes in N levels were observed when Neur was expressed (data not shown).

Neur Activity Stimulates Dl-N Signaling

Given the dramatic effect of Neur on Dl levels and subcellular localization, we decided to study its effect on the ability of Dl to signal. This can best be assayed in the larval wing pouch, where N signaling is known to induce a number of target genes including *vg*, *wingless* (*wg*), *cut* (*ct*), and *E(spl)* (Doherty et al., 1996). Furthermore, Notch is differentially glycosylated in the ventral versus dorsal wing compartments, making it preferentially responsive to Dl dorsally and preferentially responsive to Ser ventrally (Blair, 2000). We expressed *UAS-Dl* together with *UAS-GFP* (control) or with *UAS-neur* in *act>>Gal4* FLP-out clones and monitored expression of the downstream target gene product Wg (Figures 4A and 4B). The *Dl+GFP* combination gave the expected result, namely Wg expression induced in cells adjacent to clone borders in a nonautonomous fashion. Only cells adjacent to dorsal clones showed Wg expression, with the magnitude of induction gradually dropping with increased distance from the DV boundary. In contrast, coexpression of *Dl* with *neur* resulted in intense nonautonomous Wg induction adjacent to all wing pouch clones, regardless of compartment or distance from the DV boundary, suggesting that Dl signaling had been intensified to overcome compartmental limitations. Similar results were obtained when *Dl* (+*GFP* or +*neur*) was overexpressed under *omb-Gal4* control and various Notch target genes were assayed, such as *ct*, *E(spl)*, *vgBE-lacZ* (the DV boundary-specific enhancer of *vg*), and *wg* (Figures 4C and 4D; Supplemental Figures S2 and S3 [complementing Figure 4]; data not shown). In these experiments, we observed that, in addition to overcoming compartmental limitations, some Wg expression occurred within the *omb-Gal4* (Dl) expression domain. As the inability of a cell to receive Dl signal depends on its endogenous level of Dl expression (Doherty et al., 1996; Jacobsen et al., 1998), the autonomous Wg activation observed within the Dl+Neur expression domain is probably due to the dramatic lowering of Dl protein levels in those cells.

***neur* Exhibits Non-Cell-Autonomous Function during Lateral Inhibition**

Given that Neur enhances Dl signaling capacity, it is not surprising that loss of *neur* compromises the process of lateral inhibition (Lehman et al., 1983). Because the direct effects we observe are on the ligand rather than the receptor of the N signal, we would predict that the defect in lateral inhibition would be non-cell autonomous; however, recent reports have suggested an autonomous role for *neur* (Lai and Rubin, 2001; Yeh et al., 2000). To address this apparent discrepancy, we examined the effects of *neur* lof clones on development of the chemosensory SOPs of the larval wing margin, which arise in a regularly spaced pattern from two contiguous proneural clusters during the third larval instar.
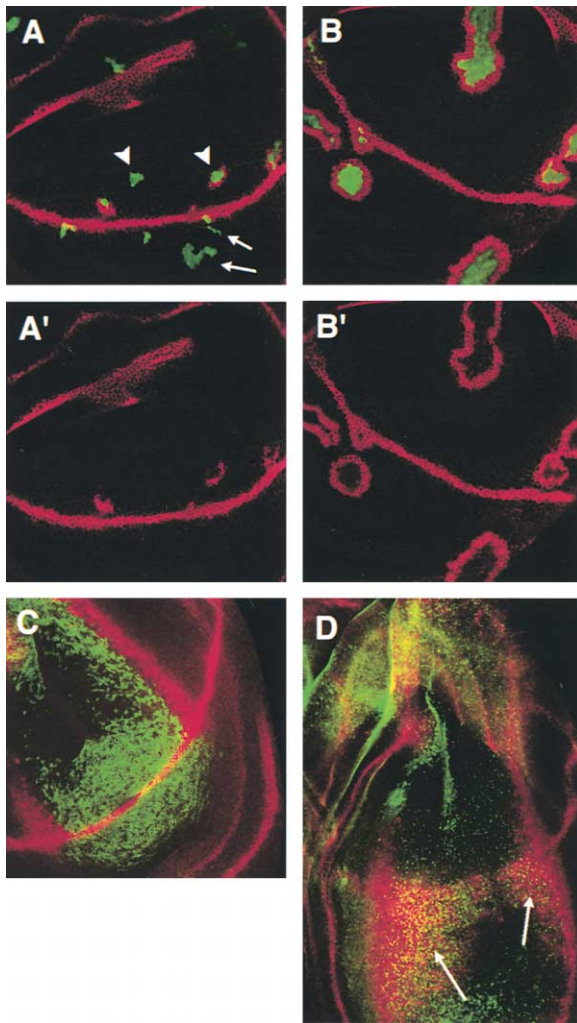
Figure 4. Effects of *neur* Overexpression on N Signaling

(A and B) Wing pouch FLP-out clones expressing *Dl* (A) or *Dl+neur* (B) are stained for Wg (red) as a read-out of N activity. GFP marks the clones.

(A) Ventral clones (arrows) or dorsal clones away from the DV boundary (arrowheads) do not turn on Wg, or do so only around part of the clone.

(B) In contrast, Wg is turned on by all *Dl+neur*-expressing clones. The same increase in Wg expression was observed upon coexpression of *Dl+neur* without *GFP*, showing that it is not an artifact due to *UAS* dosage.

(A′ and B′) Wg channel only.

(C) *omb-Gal4; UAS-Dl UAS-GFP* wing disk stained for Wg (red) and Dl (green).

(D) *omb-Gal4; UAS-Dl UAS-neur* wing disk stained as in (C). Here the Dl staining is faint and disperse due to increased internalization. Note that whereas in (C) there is no overlap between Dl and Wg, in (D) there is substantial overlap in the V compartment (arrows). Also note the increased overgrowth: (D) is at 67% the magnification of (A–C).
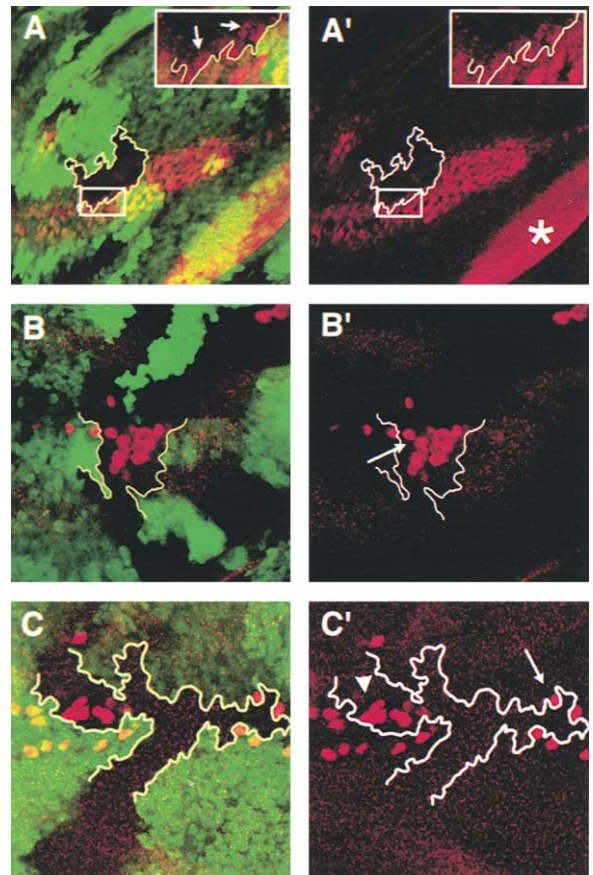

Figure 5. *neur⁻* Affects Lateral Inhibition Nonautonomously

Mutant clones are analyzed in the third instar anterior wing margin; clones are marked by the absence of GFP (green).

(A) *neur⁻* clone stained for E(spl) proteins (red, shown separately in [A′]), as a read-out of N signaling. Although overall E(spl) protein accumulation is lost within the clone (outlined), mutant cells immediately adjacent to the clone boundary within the region of neural competence do express E(spl). Inset shows higher magnification of boxed region; arrows point to some *neur⁻* cells that express E(spl). The asterisk indicates background staining.

(B and C) SOPs are visualized using anti-Ase (red, shown separately in [B′] and [C′]).

(B) A *neur⁻* clone that straddles the DV boundary is shown. Mutant cells immediately adjacent to the clone boundary can be inhibited from adopting the SOP fate, as they do not turn on Ase (arrow).

(C) *Dl^rev10* clone stained for Ase; where the clone crosses the boundary, no SOPs are seen, as the wing margin organization is disrupted. However, when the clone is only in the dorsal compartment, over-commitment of SOPs is seen (arrowhead), as in a *neur⁻* clone (B). In one part of the clone (arrow), the surrounding wt SOPs have completely inhibited SOP generation by the *Dl⁻* cells (nonautonomy). Elsewhere, a mutant SOP (arrowhead) is adjacent to wild-type non-SOP territory, an apparently autonomous arrangement. In all panels, anterior is left and dorsal is up.

We were able to focus on lateral inhibition because loss of *neur* does not affect wing margin establishment (Lai and Rubin, 2001; our unpublished observations). The *E(spl)* genes are direct transcriptional targets of N signaling during lateral inhibition. Using the mAb323, which detects five of the E(spl) bHLH proteins (Jennings et al.,

1994), we observed overall loss of E(spl) within *neur¹* clones (Figure 5A), in agreement with a defect in lateral inhibition. Still, E(spl) expression was detected in *neur⁻* cells, when the latter were adjacent to wild-type (wt) cells (Figure 5A). This implies that *neur⁻* cells are not defective in receiving signals sent by wt cells.

To further investigate the ability of *neur⁻* cells to receive N signal, we scored the disposition of SOPs (detected by Asense immunoreactivity; Brand et al., 1993)
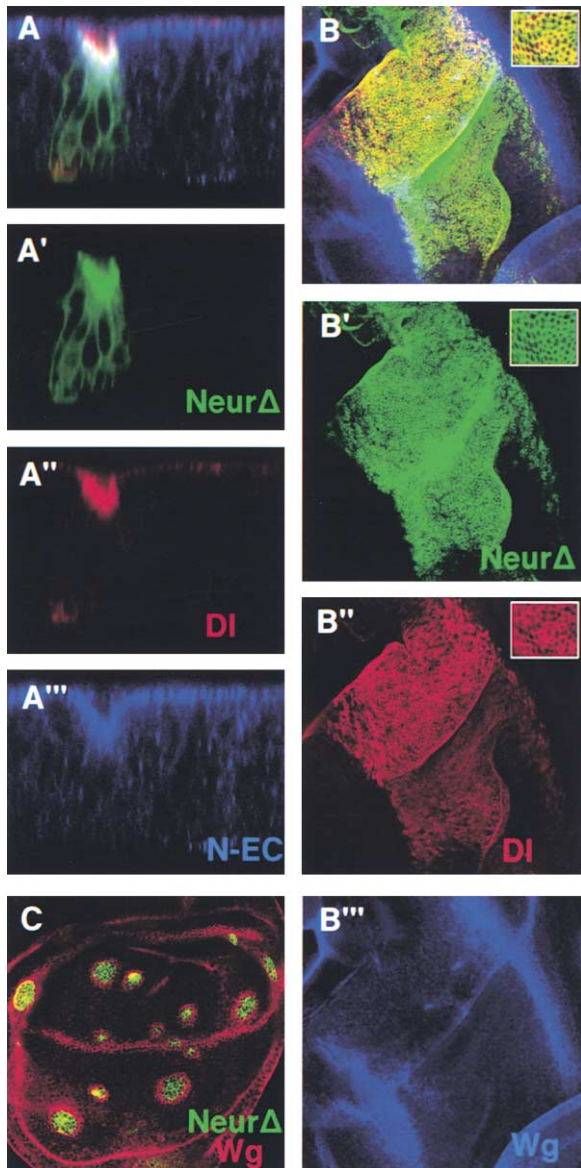
Figure 6. Effects of NeurΔRING on Dl Localization and Signaling

(A) FLP-out clone of *UAS-Dl UAS-neurΔRING-GFP* seen in cross-section (green, GFP; red, Dl; blue, N-EC; shown separately in [A'], [A''], and [A''']], respectively). All three proteins accumulate at the apical plasma membrane, with NeurΔRING-GFP showing some additional cytoplasmic localization (A').

(B) *omb-Gal4; UAS-Dl UAS-neurΔRING-GFP* third instar wing disk stained for Dl (red, [B'']) and Wg (blue, [B''']). NeurΔRING-GFP (B'). N signaling is stimulated, as Wg expression (blue, [B''']) is induced in the ventral compartment (cf. Figure 4C). This induction is more spatially restricted than that caused by wt Neur (cf. Figure 4D).

(C) *act>>Gal4; UAS-Dl UAS-neurΔRING-GFP* FLP-out clones stained for Wg (red). Wg induction is induced (nonautonomously) in both dorsal and ventral compartments (cf. Figures 4A and 4B).

relative to clone borders. If loss of *neur* affected signal sending rather than receiving, we would expect to encounter *neur⁻* cells that are inhibited, that is, do not become SOPs, next to wt SOPs at clone borders. This nonautonomous arrangement was observed in 24 cases (60% of the clone borders scored; Figure 5B), whereas

the converse "autonomous" arrangement (wt non-SOP next to *neur* SOP) was observed in only seven cases (18%). The remaining nine clone borders (23%) showed adjacent wt and *neur⁻* SOPs. These could be interpreted either as inability of the *neur⁻* SOP to send signal (thereby not inhibiting its neighboring wt cell) or its inability to receive signal (thereby not becoming laterally inhibited by the neighboring wt SOP). Scoring of *Dl⁻* clone borders (Figure 5C), as a bona fide non-cell-autonomous control, yielded a predominance of the nonautonomous arrangement in agreement with Heitzler and Simpson (1991): 29 wt SOPs next to *Dl⁻* non-SOPs (83% nonautonomous) versus five *Dl⁻* SOPs next to wt non-SOPs (14% autonomous), and almost no pairs of wt mutant SOPs at the border (one case; 3%). *N⁻* clones, by contrast, produced the autonomous arrangement in 98% of clone borders (Heitzler and Simpson, 1991). Thus, *neur⁻* clones behave more like *Dl⁻* clones than like *N⁻* clones, arguing for a nonautonomous action of Neur. The somewhat lower incidence of nonautonomy in *neur⁻* clones compared to *Dl⁻* clones may be due to an early bias of *Dl⁻* cells to become inhibited by their wt neighbors (Heitzler and Simpson, 1991). As this bias probably arises before onset of *neur* expression in the nascent SOP, it cannot be expected to occur in *neur⁻* clones.

The Neur RING Domain Is Required for Dl Internalization but Is Dispensable for Dl Signaling

Although the biochemical function of Neur remains to be elucidated, the protein contains a RING domain, which has been associated with E3 ubiquitin ligase activity in other proteins (Freemont, 2000). Because ubiquitination is known to regulate endocytic events (Di Fiore and De Camilli, 2001), we asked whether a mutant lacking the RING would be defective in stimulating Dl internalization. We substituted the RING domain with a GFP moiety, in order to additionally monitor the localization of the protein. The tagged mutant protein accumulated at the apical plasma membrane (Figures 6A and 6B), which is where wt Neur has been reported to localize (Lai and Rubin, 2001; Yeh et al., 2000). This suggests that the RING is dispensable for membrane localization.

Despite the correct subcellular localization of NeurΔRING-GFP, its coexpression with *UAS-Dl* resulted in retention of Dl at the apical membrane, comparable to that observed when expressing *UAS-Dl* alone (Figures 6A and 6B). The RING domain is, therefore, required for Dl internalization. The lack of internalization was accompanied by lack of turnover. Coexpression of *Dl* and *neurΔRING-GFP* led to accumulation of the full-length Dl isoform to a level comparable to that associated with expression of *Dl* alone, whereas accumulation of the cleaved isoform was reduced by about 50% (Figure 3). We next assessed Wg expression to determine the extent to which the mutant Neur was able to stimulate Dl signaling. To our surprise, coexpression of Dl with NeurΔRING-GFP was still able to stimulate Wg expression in both compartments of the wing in a nonautonomous fashion (Figures 6B and 6C; Supplemental Figure S4 [complementing Figure 6]). The only difference between wt Neur and NeurΔRING-GFP in this assay was
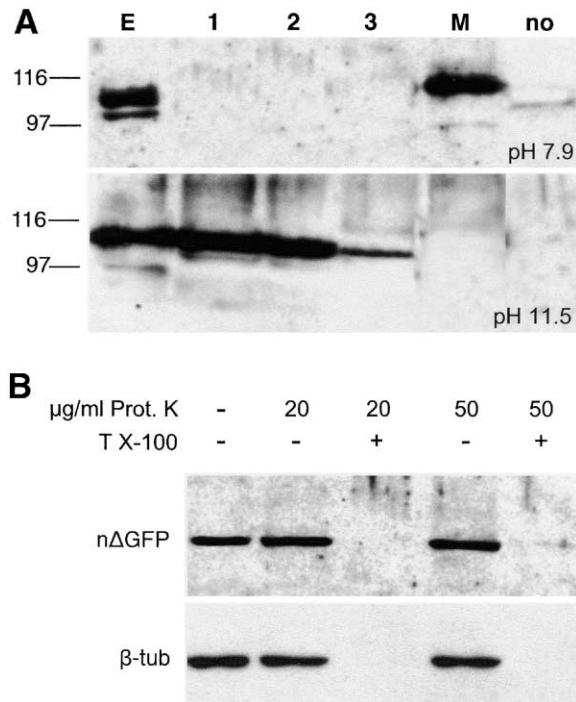
Figure 7. NeurΔRING-GFP Is an Intracellular Peripheral Membrane Protein

(A) Subcellular fractionation of *hs-Gal4; UAS-neurΔRING-GFP* larvae was performed after lysis in a hypotonic buffer (top panel) or by high pH (bottom panel). GFP is visualized by immunoblotting. Lane E: crude extract; lanes 1, 2, and 3: soluble fractions after successive washes; lane M: insoluble "membrane" fraction; lane no: no heat shock control crude extract.

(B) NeurΔRING-GFP is protected from proteinase K digestion in intact tissue. Total extracts of *omb-Gal4; UAS-neurΔRING-GFP* wing disks. Each sample was treated as indicated before lysis. Western blot with anti-GFP antibody (top panel) or with anti-β-tubulin antibody (bottom panel).

the inability of the latter to overcome the cis-dominant-negative effect of Dl, when expressed under *omb-Gal4* (compare Figure 6B with Figure 4D).

NeurΔRING-GFP Is an Intracellular Peripheral Membrane Protein

As the Neur sequence does not contain any obvious signal peptide or transmembrane domain, we undertook a biochemical approach to determine the type of association Neur might have with the membrane. Extracts from larvae ubiquitously expressing *UAS-neurΔRING-GFP* were fractionated by ultracentrifugation and the GFP-tagged Neur was detected by immunoblotting. Under mild extraction conditions, NeurΔRING-GFP was found in the membrane fraction, consistent with histological observations. However, following extraction with high pH, which strips membranes of all but integral proteins (Fujiki et al., 1982), NeurΔRING-GFP was detected exclusively in the cytosolic fraction, suggesting a peripheral association with the membrane (Figure 7A). This association must occur on the cytoplasmic face of the cell membrane, as Neur contains no signal peptide. To test this hypothesis, we isolated wing disks overexpressing *UAS-neurΔRING-GFP* and subjected them to proteinase K digestion before lysis and immunoblotting. The GFP (NeurΔRING-GFP) immunoreactivity was resistant to the membrane-impermeable proteinase K, supporting the assignment to Neur of an intracellular location (Figure 7B). We believe that the wt Neur protein, which is known to associate with the membrane (Lai and Rubin, 2001; Yeh et al., 2000), will also have the same topology, because the RING domain should not act as a transmembrane domain.

Discussion

The importance of *neur* in N signaling has been realized ever since its identification, as its null embryonic phenotype is indistinguishable from that of *N* mutants (Lehman et al., 1983). Nonetheless, its position in the N pathway was heretofore unclear. Our analysis of *neur* loss of function (lof) and overexpression suggests a link between *neur* expression and Dl signaling and endocytosis. Loss of *neur* diminishes Dl endocytosis, whereas *neur* ectopic expression enhances Dl endocytosis and turnover. While this manuscript was under review, a paper by Yeh et al. (2001) reported that Neur indeed has RING-dependent E3 ubiquitin ligase activity in vitro. Taken together, our data and those of Yeh et al. (2001) link Dl endocytosis with ubiquitination, as originally hypothesized (see Results).

One caveat to our interpretation is that our static pictures of Dl localization do not allow us to unambiguously conclude whether intracellular Dl is endocytosed or blocked in its secretory trafficking. We favor the former hypothesis for three reasons: (1) intracellular Dl often colocalizes with endocytosed fluorescent dextran; (2) if Dl were retained in the endoplasmic reticulum or Golgi, it would not be available at the cell surface where signaling is taking place; yet, concomitant with increased endocytosis, Neur is able to stimulate Dl signaling; and (3) wt Neur protein is found mostly at the plasma membrane (Lai and Rubin, 2001; Yeh et al., 2000), so it is more likely to affect endocytic events rather than steps in secretory processes.

The nonautonomous effect of *neur⁻* clones on lateral inhibition (Figure 5) favors a role for Neur in signal-emitting, rather than signal-receiving, cells. Such a function is consistent with the fact that Neur is an intracellular peripheral membrane protein expressed preferentially in the signal-emitting cells during lateral inhibition, such as the neuroblasts, SOPs, and central provein cells (Boulianne et al., 1993; Huang et al., 1991; this work). In agreement with a role for Neur in generating the Dl signal, prior epistasis analysis showed that *neur* is required to express the embryonic neural suppression ("antineurogenic") phenotype associated with ligand-dependent *N* gain-of-function (gof) mutants (Lieber et al., 1993). In the same study, *neur* was dispensable for the constitutive activity of ligand-independent N variants. Interestingly, some N variants that are *Dl* independent are also *shi* (Dynamin) independent (Seugnet et al., 1997; Struhl and Adachi, 2000). Taken together, these data point to the involvement of Neur and Dynamin in processes upstream of (or parallel to) N activation by Dl. Our implication of Neur in endocytic regulation suggests an important role for endocytosis in events leading

up to N activation (Parks et al., 2000; Seugnet et al., 1997).

If Dl endocytosis and Dl-N signaling are causally linked, then our analysis of the NeurΔRING-GFP mutant poses a paradox: although NeurΔRING-GFP does not detectably stimulate Dl endocytic trafficking (or turnover), it retains the ability to enhance Dl signaling. On the one hand, this could mean that the above model is wrong and endocytosis is simply a consequence of Dl-N stimulation, rather than a prerequisite for Dl signaling. Alternatively, the absence of detectable Dl internalization upon coexpression of NeurΔRING-GFP does not necessarily preclude the possibility that early endocytic events (e.g., recruitment of Dl into coated pits) that are undetectable by light microscopy are initiated by NeurΔRING-GFP. Such events might be sufficient to stimulate ligand-dependent N cleavage and activation. Ultrastructural analysis will be required to distinguish between these alternative models.

Removal of the Neur RING domain does seem to adversely affect its ability to stimulate N signaling in some contexts: in the study of Lai and Rubin (2001), *UAS-neurΔRING* yielded phenotypes indicative of a negative effect on N signaling (tufted bristles, thick veins, and notched wings) with most *Gal4* driver lines, although in certain cases, positive effects were also observed (shaft to socket transformation). We have observed the same context-dependent variability with our *UAS-neurΔRING-GFP* construct (data not shown), suggesting that these differences do not result from the presence of the GFP moiety but rather from the type of assay employed. In fact, we have shown that NeurΔRING-GFP coexpressed with Dl blocks N signaling within the *omb-Gal4* domain, where wt Neur and Dl are able to induce Wg, even though the nonautonomous signaling (at the borders of the *omb-Gal4* domain or at the borders of FLP-out clones) appears unaffected by the RING deletion (Figures 6B and 6C). It is possible then that NeurΔRING can exert negative effects on Dl-N signaling in a cell-autonomous fashion and positive effects in a cell-non-autonomous fashion. The cell-autonomous block in N signaling could be due to the block in Dl turnover and its accumulation at the apical membrane, because it has been proposed that high levels of Dl may sequester N receptor molecules in unproductive cis complexes (Jacobsen et al., 1998).

Two major models for Dl signaling have been put forward. In one, the active Dl species is proposed to be the extracellularly cleaved, secreted Dl-EC fragment (Qi et al., 1999), because it is produced by the metalloprotease Kuzbanian (Kuz), and the *kuz* lof phenotype is similar to the *N* lof phenotype (Rooke et al., 1996). In the other, binding of cell surface-tethered Dl to N on the apposing cell has a dual impact: activating extracellular cleavage of Notch and mediating the transendocytosis into the signal-sending cell of N-EC complexed with Dl (Parks et al., 2000). Our observations suggest that Neur could act intracellularly in the signal-sending cell to promote assembly of a productive Dl-N complex and to trigger its endocytosis. Concomitantly with endocytosis, Neur leads to a drastic reduction in the levels of the Dl-EC fragment (Figure 3), even as Dl-N signaling is increased. It therefore appears unlikely that Dl-EC is the active signal that stimulates N in the wing disk. This

leaves unanswered at present the question of why Kuz is needed for N signaling. Perhaps Kuz has pleiotropic activity and acts on some other protein(s) required for N activation, and Kuz-dependent Dl cleavage is a secondary effect. Better characterization of the different Dl isoforms, including their localization and trafficking, will be required to understand the detailed mechanism of Dl-N activation.

Despite the proposed role of Neur to promote Dl signaling, we also note that Dl can signal in the absence of Neur, inasmuch as there are instances of Dl signaling where Neur is not detectably expressed, such as from the germline to ovarian follicle cells (Lopez-Schier and St Johnston, 2001). In the experiments of Figures 4A and 4C, we indeed observed N target gene expression induced by Dl in the absence of *neur*. To be certain, we monitored *neur*[A101]-*lacZ* and showed that *UAS-Dl* overexpression in the wing disk does not induce endogenous *neur* expression (data not shown). With the caveat that available detection methods may fail to detect low levels of *neur* expression, we propose that two types of Dl signaling may exist: basal signaling that does not require Neur activity and high-intensity signaling that does. During neurogenesis, basal Dl-N signaling probably takes place during early stages among all cells within proneural clusters, where Dl and N are uniformly expressed but Neur is absent. Upon expression of *neur* by a nascent neural precursor, signaling becomes asymmetric, as the neighboring cells receive more intense signal even though Dl and N levels have not changed. The absolute requirement for *neur* in neurogenesis suggests that basal "mutual" inhibition is insufficient to permanently block proneural protein activity. Indeed, the E(spl) bHLH Notch targets, which are the main antagonists of proneural proteins, are not expressed in *neur*⁻ embryos (Jennings et al., 1994) or clones (Figure 5A), suggesting that their expression may be induced only by intense Neur-dependent "lateral" inhibitory signaling.

We can extend our hypothesis to propose that Neur may be required more stringently in instances in which a novel asymmetry has to be imposed upon uniform basal N-Dl signaling. *neur* is not required at the wing DV boundary (Lai and Rubin, 2001; our unpublished observations), where asymmetry is imposed by Fringe (Blair, 2000) or in the egg chamber, where asymmetry is imposed by expression of N and Dl in distinct cells (Lopez-Schier and St Johnston, 2001). Similarly, *neur* is not essential during lateral inhibition within the provein. Despite its expression there and its dramatic effect on Dl localization (Figure 1G), *neur* lof clones yield normal looking veins with only minor thickenings (Lai and Rubin, 2001; our unpublished observations). We believe that *neur* is not crucial for this process because wing patterning mechanisms place N and Dl in different cells: Dl expression is most intense within the central proveins and N expression is most intense within the lateral proveins (de Celis et al., 1997; Huppert et al., 1997).

Although the exact relationship between Dl endocytosis and N activation remains to be resolved, our findings emphasize the importance of Neur for both of these processes. Given the complexity and pleiotropy of Notch signaling, alternative mechanisms of signal generation may be operative in different developmental contexts. The questions of whether this is so, and if so,

what mechanisms operate in which contexts, will be resolved by future work.

Experimental Procedures

Antibodies and Immunohistochemistry

For antibody staining, dissected larvae were fixed for 20 min at room temperature in PEM plus 4% formaldehyde. Pupal dissection and fixation was done as in Parks et al. (2000). To induce the *hs-GFP* marker, 1 hr of heat shock at 38°C and 1–1.5 hr recovery was done prior to dissection. Dl was detected using mouse mAb C594.9B (Fehon et al., 1990) at 1:5,000 or guinea pig serum GP581 (Huppert et al., 1997) at 1:4,000, both directed against extracellular epitopes. N was detected using mouse mAb C458.2H (Diederich et al., 1994) supernatant at 1:100, also recognizing an extracellular epitope. Fasciclin III was detected using mAb 7G10 (Developmental Studies Hybridoma Bank; developed under the auspices of the NICHD and maintained by the University of Iowa, Department of Biological Sciences, Iowa City) supernatant at 1:500. For β-galactosidase, we used a rabbit antiserum from Cappel (1:10,000). mAbs against Ct (1:100), Wg (1:10), and E(spl) (1:3) were kindly provided by Karen Blochlinger (FHCRC, Seattle), Stephen Cohen (EMBL, Heidelberg), and Sarah Bray (University of Cambridge, UK), respectively. Rabbit anti-Ase serum (1:1,000) was kindly provided by Andrew Jarman (University of Edinburgh). Fluorescent and HRP-coupled secondary antibodies were from Jackson Immunochemicals or Molecular Probes. They were preadsorbed and used at 1:200–1:1,000. Antibody incubations were done in PBS/0.2% Triton/0.5% BSA at 4°C for 4 hr to overnight. Fluorescent samples were observed using a Leica SP confocal microscope. Transmitted light images were obtained on a Leica Diaplan microscope.

Mosaic Analysis

Mitotic clones were induced using the *FLP-FRT* technique. Flies were raised at 25°C and *hsFLP* was induced by heat-shocking first to second instar larvae of the following genotypes for 1 hr at 38°C: (1) *y w hsFLP/ w; FRT82B neur¹/ FRT82B hsGFP or FRT82B arm-lacZ;* (2) *y w hsFLP/ w; FRT82B Dl^{rev10}/ FRT82B hsGFP;* and (3) *y w hsFLP/ w; FRT82B P[gro⁺] Df(3R)b32.2/ FRT82B hsGFP.*

FRT82B stands for *P[neoFRT]82B* and *hsFLP* stands for *P[hsFLP]1*. All alleles and inserts shown above are described in FlyBase (http://flybase.bio.indiana.edu). The *FRT82B P[gro⁺] Df(3R)b32.2* chromosome (kindly provided by Pat Simpson) carries a *P[gro⁺]* transgene to complement the partial inactivation of *gro* by the deficiency for the *E(spl)* locus.

Constructs and Transgenic Lines

UAS-neur was constructed as follows: a DraI fragment was isolated corresponding to nucleotides 247–2637 of the *neur* cDNA (includes 30 bp of 5′ UTR and 95 bp of 3′ UTR) and cloned into the EcoRV site of pBluescript KSII+ (Stratagene) to generate pBNeur. A BamHI-KpnI (polylinker sites) fragment from pBNeur was isolated and cloned into pUAST cut with BglII and KpnI.

UAS-neurΔRING-GFP was constructed as follows: a BamHI (polylinker)-HincII (*neur* cDNA nucleotide 2146) fragment was isolated from pBNeur and cloned into the pEGFP-N2 vector (Clontech) cut with BglII and SmaI, fusing the first 623 amino acids of Neur in-frame with *EGFP*. The chimeric *neur-EGFP* fragment was isolated from this plasmid by SmaI-NotI (polylinker sites) and cloned into pUAST cut with EcoRI/filled-in and NotI. Transgenic lines were generated in a *yw^{67c23}* background.

Other transgenes used were *P[lArB]neur^{A101}* (*neur^{A101}-lacZ*), *P[lArB]Dl^{A326.2F3}* (*Dl-lacZ*), and *P[lacZ]N^{MLz}* (*N-lacZ*), all described in FlyBase. *UAS-Dl* was kindly provided by Nick Baker (Albert Einstein College of Medicine, New York).

Targeted Gene Expression

The following *Gal4* drivers were used: *P[GAL4]bi^{omb-Gal4}*, *act>CD2>Gal4* (FlyBase: *P[GAL4-Act5C(FRT.CD2).P]S*), *P[GAL4]neur^{GAL4-A101}* (kindly provided by Veronica Rodrigues, Bombay), and *P[GAL4-Hsp70.sev]K25* (*hs-Gal4*). All crosses were performed at 25°C. For the FLP-out clones larvae carrying the *act>CD2>Gal4* line, *P[hsFLP]1* and a *UAS* transgene were heat-shocked for 30 min at 37°C to induce the clonal elimination of the *CD2* cassette by FLP-mediated intramolecular recombination between the two *FRT* sites (>). This juxtaposes the *Act5C* promoter to *Gal4* and drives *UAS* transgene expression at a low uniform level in all cells of the clone.

Endocytosis Assay

Dissected third instar larval disc complexes were incubated in 1 mM fluorescein-dextran/lysine-fixable, MW 3,000 (Molecular Probes) in M3 cell culture medium at 25°C for 10 min (pulse), and then washed five times in ice-cold M3 medium. After a variable chase period (0–60 min), they were fixed in PEM plus 4% formaldehyde. Dextran is taken up by endocytosis and marks progressively later endosomal compartments as the chase time is increased (Entchev et al., 2000).

Protein Analysis

For the Dl Westerns, wing disks of the appropriate genotypes were collected in ice-cold PBS and subsequently extracted in a buffer consisting of 300 mM NaCl, 50 mM Tris (pH 8.0), 0.5% NP-40, 1 mM CaCl₂, 1 mM MgCl₂, and protease inhibitors. Laemmli gels were run in the absence of reducing agents. Dl was detected on a Western blot using mAb C594.9B at 1:10,000. N-EC was detected using the same conditions and the C458.2H mAb at 1:1,000. N-IC was detected using reducing conditions and the C17.9C6 mAb at 1:5,000 (Fehon et al., 1990). We used anti-β-tubulin mAb (Amersham) at 1:4,000 as a loading control. The HRP-coupled goat anti-mouse IgG (Jackson Immunochemicals) was used at 1:10,000 and the blots were developed using a chemiluminescent substrate (Pierce).

For the subcellular fractionation analysis, we used *hs-Gal4; UAS-neurΔRING-GFP* third instar larval brain disk complexes. The larvae had been heat-shocked for 1 hr at 38°C to induce the transgene and returned to room temperature for 3 hr before dissection. To strip membranes from peripherally associated proteins, we homogenized the tissue in 100 mM Na₂CO₃ (pH 11.5) (Fujiki et al., 1982) in the presence of protease inhibitors. After a 45 min incubation at 4°C, we separated the membrane and cytosolic fractions by ultracentrifugation (68,000 rpm in TLA-120 rotor, Beckman ultramicrocentrifuge). For mild lysis, we used the same procedure, changing the lysis buffer to a hypotonic one, 25 mM HEPES (pH 7.9), 1.5 mM MgCl₂, and 10 mM KCl. We detected the NeurΔRING-GFP protein by Western blot (as above) using rabbit anti-GFP (Invitrogen) at 1:5,000 and HRP-coupled goat anti-rabbit IgG (Jackson Immunochemicals) at 1:15,000.

For the proteinase K protection analysis, we collected 50 third instar wing disks from *omb-Gal4; UAS-neurΔRING-GFP* animals and incubated them intact in various concentrations of proteinase K in PBS (10 min at 30°C). PMSF (3 mM) was added to stop the reaction, and the tissue was homogenized directly in 1× Laemmli sample buffer. The fusion protein and β-tubulin were detected by Western blot, as above.

References

Artavanis-Tsakonas, S., Rand, M.D., and Lake, R.J. (1999). Notch signaling: cell fate control and signal integration in development. Science *284*, 770–776.

Baker, N.E. (2000). Notch signaling in the nervous system. Pieces still missing from the puzzle. Bioessays *22*, 264–273.

Baker, N.E., and Yu, S.Y. (1998). The R8-photoreceptor equivalence group in *Drosophila*: fate choice precedes regulated Delta transcription and is independent of Notch gene dose. Mech. Dev. *74*, 3–14.

Blair, S.S. (2000). Notch signaling: Fringe really is a glycosyltransferase. Curr. Biol. *10*, R608–R612.

Boulianne, G.L., de la Concha, A., Campos-Ortega, J.A., Jan, L.Y., and Jan, Y.N. (1993). The *Drosophila* neurogenic gene neuralized encodes a novel protein and is expressed in precursors of larval and adult neurons. EMBO J. *12*, 2586.

Brand, M., Jarman, A.P., Jan, L.Y., and Jan, Y.N. (1993). *asense* is a *Drosophila* neural precursor gene and is capable of initiating sense organ formation. Development *119*, 1–17.

Brou, C., Logeat, F., Gupta, N., Bessia, C., LeBail, O., Doedens, J.R., Cumano, A., Roux, P., Black, R.A., and Israel, A. (2000). A novel proteolytic cleavage involved in Notch signaling: the role of the disintegrin-metalloprotease TACE. Mol. Cell *5*, 207–216.

de Celis, J.F., Bray, S., and Garcia-Bellido, A. (1997). Notch signalling regulates veinlet expression and establishes boundaries between veins and interveins in the *Drosophila* wing. Development *124*, 1919–1928.

Diederich, R.J., Matsuno, K., Hing, H., and Artavanis-Tsakonas, S. (1994). Cytosolic interaction between deltex and Notch ankyrin repeats implicates deltex in the Notch signaling pathway. Development *120*, 473–481.

Di Fiore, P.P., and De Camilli, P. (2001). Endocytosis and signaling. An inseparable partnership. Cell *106*, 1–4.

Doherty, D., Feger, G., Younger-Shepherd, S., Jan, L.Y., and Jan, Y.N. (1996). Delta is a ventral to dorsal signal complementary to Serrate, another Notch ligand, in *Drosophila* wing formation. Genes Dev. *10*, 421–434.

Entchev, E.V., Schwabedissen, A., and Gonzalez-Gaitan, M. (2000). Gradient formation of the TGF-beta homolog Dpp. Cell *103*, 981–991.

Fehon, R.G., Kooh, P.J., Rebay, I., Regan, C.L., Xu, T., Muskavitch, M.A.T., and Artavanis-Tsakonas, S. (1990). Molecular interactions between the protein products of the neurogenic loci *Notch* and *Delta*, two EGF-homologous genes in *Drosophila*. Cell *61*, 523–534.

Fehon, R.G., Johansen, K., Rebay, I., and Artavanis-Tsakonas, S. (1991). Complex cellular and subcellular regulation of Notch expression during embryonic and imaginal development of *Drosophila*: implications for Notch function. J. Cell Biol. *113*, 657–669.

Freemont, P.S. (2000). Ubiquitination: RING for destruction? Curr. Biol. *10*, R84–R87.

Fujiki, Y., Hubbard, A.L., Fowler, S., and Lazarow, P.B. (1982). Isolation of intracellular membranes by means of sodium carbonate treatment: applications to endoplasmic reticulum. J. Cell Biol. *93*, 97–102.

Heitzler, P., and Simpson, P. (1991). The choice of cell fate in the epidermis of *Drosophila*. Cell *64*, 1083–1092.

Huang, F., Dambly-Chaudiére, C., and Ghysen, A. (1991). The emergence of sense organs in the wing disc of *Drosophila*. Development *111*, 1087–1095.

Huppert, S.S., Jacobsen, T.L., and Muskavitch, M.A. (1997). Feedback regulation is central to Delta-Notch signalling required for *Drosophila* wing vein morphogenesis. Development *124*, 3283–3291.

Jacobsen, T.L., Brennan, K., Martinez-Arias, A., and Muskavitch, M.A. (1998). Cis-interactions between Delta and Notch modulate neurogenic signalling in *Drosophila*. Development *125*, 4531–4540.

Jennings, B., Preiss, A., Delidakis, C., and Bray, S. (1994). The Notch signalling pathway is required for *Enhancer of split* bHLH protein expression during neurogenesis in the *Drosophila* embryo. Development *120*, 3537–3548.

Klueg, K.M., Parody, T.R., and Muskavitch, M.A. (1998). Complex proteolytic processing acts on Delta, a transmembrane ligand for Notch, during *Drosophila* development. Mol. Biol. Cell *9*, 1709–1723.

Kooh, P.J., Fehon, R.G., and Muskavitch, M.A.T. (1993). Implication of dynamic patterns of Delta and Notch expression for cellular interactions during *Drosophila* development. Development *117*, 493–507.

Lai, E.C., and Rubin, G.M. (2001). *neuralized* functions cell-autonomously to regulate a subset of Notch-dependent processes during adult *Drosophila* development. Dev. Biol. *231*, 217–233.

Lehman, R., Jiménez, F., Dietrich, U., and Campos-Ortega, J.A. (1983). On the phenotype and development of mutants of early neurogenesis in *Drosophila melanogaster*. Roux's Arch. Dev. Biol. *192*, 62–74.

Lieber, T., Kidd, S., Alcamo, E., Corbin, V., and Young, M.W. (1993). Antineurogenic phenotypes induced by truncated *Notch* proteins indicate a role in signal transduction and may point to a novel function of *Notch* in nuclei. Genes Dev. *7*, 1949–1965.

Lopez-Schier, H., and St Johnston, D. (2001). Delta signaling from the germ line controls the proliferation and differentiation of the somatic follicle cells during *Drosophila* oogenesis. Genes Dev. *15*, 1393–1405.

McNiven, M.A., Cao, H., Pitts, K.R., and Yoon, Y. (2000). The dynamin family of mechanoenzymes: pinching in new places. Trends Biochem. Sci. *25*, 115–120.

Mumm, J.S., and Kopan, R. (2000). Notch signaling: from the outside in. Dev. Biol. *228*, 151–165.

Neumann, C.J., and Cohen, S.M. (1998). Boundary formation in *Drosophila* wing: Notch activity attenuated by the POU protein Nubbin. Science *281*, 409–413.

Parks, A.L., Turner, F.R., and Muskavitch, M.A. (1995). Relationships between complex Delta expression and the specification of retinal cell fates during *Drosophila* eye development. Mech. Dev. *50*, 201–216.

Parks, A.L., Klueg, K.M., Stout, J.R., and Muskavitch, M.A. (2000). Ligand endocytosis drives receptor dissociation and activation in the Notch pathway. Development *127*, 1373–1385.

Poodry, C.A. (1990). shibire, a neurogenic mutant of *Drosophila*. Dev. Biol. *138*, 464–472.

Price, B.D., Chang, Z., Smith, R., Bockheim, S., and Laughon, A. (1993). The *Drosophila* neuralized gene encodes a C3HC4 zinc finger. EMBO J. *12*, 2411–2418.

Qi, H., Rand, M.D., Wu, X., Sestan, N., Wang, W., Rakic, P., Xu, T., and Artavanis-Tsakonas, S. (1999). Processing of the Notch ligand Delta by the metalloprotease Kuzbanian. Science *283*, 91–94.

Rand, M.D., Grimm, L.M., Artavanis-Tsakonas, S., Patriub, V., Blacklow, S.C., Sklar, J., and Aster, J.C. (2000). Calcium depletion dissociates and activates heterodimeric notch receptors. Mol. Cell. Biol. *20*, 1825–1835.

Rooke, J., Pan, D., Xu, T., and Rubin, G.M. (1996). KUZ, a conserved metalloprotease-disintegrin protein with two roles in *Drosophila* neurogenesis. Science *273*, 1227–1231.

Seugnet, L., Simpson, P., and Haenlin, M. (1997). Requirement for dynamin during Notch signaling in *Drosophila* neurogenesis. Dev. Biol. *192*, 585–598.

Speicher, S.A., Thomas, U., Hinz, U., and Knust, E. (1994). The *Serrate* locus of *Drosophila* and its role in morphogenesis of the wing imaginal discs: control of cell proliferation. Development *120*, 535–544.

Struhl, G., and Adachi, A. (2000). Requirements for presenilin-dependent cleavage of notch and other transmembrane proteins. Mol. Cell *6*, 625–636.

Yeh, E., Zhou, L., Rudzik, N., and Boulianne, G.L. (2000). Neuralized functions cell autonomously to regulate *Drosophila* sense organ development. EMBO J. *19*, 4827–4837.

Yeh, E., Dermer, M., Commisso, C., Zhou, L., McGlade, C.J., and Boulianne, G.L. (2001). Neuralized functions as an E3 ubiquitin ligase during *Drosophila* development. Curr. Biol. *11*, 1675–1679.